Experimental Study on Online Demagnetization of High-Q SHINE Modules

Authors: Dr. YongZhou He, Dong, Mr. Jian, He, Dr. YongZhou

Date: 2025-05-28T15:18:07+00:00

Abstract

Cryogenic modules are key equipment systems in SHINE. To achieve a high quality factor Q0 for the superconducting cavities in cryogenic modules, it is essential to create a low-magnetic-field operating environment. Efficient magnetic shielding for superconducting cavities effectively shields against background magnetic fields; excessive background magnetic fields significantly reduce the effectiveness of cryogenic Permalloy magnetic shielding. During manufacturing, installation, integration, test, and transportation, cryogenic modules generate residual magnetic fields B of varying degrees, necessitating online in-situ precision demagnetization of the entire cryogenic module to reduce the background magnetic field for magnetic shielding. Taking the SHINE cryogenic module as an example, this paper introduces the online in-situ demagnetization of the entire cryogenic module and analyzes the experimental results. The study shows that after online demagnetization of the entire SHINE module, the magnetic field B inside the superconducting cavity is less than 1.0 mGs when the superconducting cavity Q0 reaches 2.7 × 1010 to 5.0 ×1010. The research results provide a reference for the demagnetization of cryogenic modules in similar FEL free-electron laser facilities worldwide.

Full Text

Experimental Study on Online Demagnetization of High-Q SHINE Modules

Yong-zhou He[1],† and Jian Dong[1]
[1]Shanghai Advanced Research Institute, Chinese Academy of Sciences, Shanghai, 201204, China

Cryogenic modules are key equipment systems in SHINE. To achieve a high quality factor Q for the superconducting cavities in these modules, it is essential to create a low-magnetic-field operating environment. While efficient

magnetic shielding for superconducting cavities effectively shields against background magnetic fields, excessive background fields significantly reduce the effectiveness of cryogenic Permalloy magnetic shielding. During manufacturing, installation, integration, testing, and transportation, cryogenic modules generate residual magnetic fields B of varying degrees, necessitating online in-situ precision demagnetization of the entire cryogenic module to reduce the background magnetic field for magnetic shielding. Taking the SHINE cryogenic module as an example, this paper introduces the online in-situ demagnetization of the entire cryogenic module and analyzes the experimental results. The study shows that after online demagnetization of the entire SHINE module, the magnetic field B inside the superconducting cavity is less than 1.0 mGs when the superconducting cavity Q reaches 2.7×10^{1} to 5.0×10^{1}. These research results provide a reference for the demagnetization of cryogenic modules in similar FEL free-electron laser facilities worldwide.

Keywords: cryogenic module, whole machine demagnetization, weak magnetic field, quality factor Q

INTRODUCTION

The Hard X-ray Free Electron Laser Facility (SHINE) is planned to operate 75 complex large-scale cryogenic superconducting accelerator modules, which include 600 standard 1.3 GHz high-Q radio-frequency superconducting cavities [1–3]. To achieve the design value of the quality factor Q of 2.70×10^{1} at 16 MV/m for the standard 1.3 GHz module superconducting cavities, reduce the thermal load on the SHINE cryogenic refrigeration system, and save costs in construction, equipment development, integration test, and operational maintenance, it is necessary to provide a weak magnetic field operating environment for these cavities [4–6]. The smaller the residual magnetic induction B (referred to as residual magnetic field B) inside the superconducting cavities, the higher the Q will be [7–9], as shown in Fig. 1 [FIGURE:1].

It can be observed that when the residual magnetic field B inside the superconducting cavity is controlled to approximately 3.00 mGs, the Q of the superconducting cavity can reach 2.7×10^{1} [10–12]; if the residual magnetic field B is controlled to 0.50 mGs, the Q of the superconducting cavity can approach 4.0×10^{1}. According to the SHINE high-Q module whole machine online demagnetization technical standards, after online demagnetization of the standard 1.3 GHz module, the magnetic field detection indicators for the two fluxgate probes between the magnetic shielding layers are as follows: (1) At the ground-level horizontal test position, the average absolute value of the two fluxgate probes is less than 0.60 mGs. (2) At the underground tunnel operating position, the average absolute value of the two fluxgate probes is less than 1.00 mGs.

The weak magnetic field environment for superconducting cavities is closely related to the effectiveness of magnetic shielding. "Magnetic shielding" is made

from high-permeability magnetic materials, such as sheets formed into geometric shapes like spherical rings, frames, or cylinders, to "divert" nearby magnetic field lines and achieve a clean background magnetic field. The design principle of low-frequency static magnetic field shielding is to use high magnetic permeability materials like pure iron, silicon steel, and Permalloy to shunt the interfering magnetic fields (see Fig. 2(a) [FIGURE:2]), thereby significantly reducing the residual magnetic field in the working area of the equipment [13]. From the principles of static magnetic field shielding, the following conclusions can be drawn: First, the higher the permeability μ of the ferromagnetic material and the larger the cross-sectional area s of the magnetic shielding structure, the smaller the magnetic reluctance R of the magnetic circuit. Consequently, the magnetic flux Φ concentrated in the magnetic circuit is greater, and the leakage magnetic flux Φ in the air is significantly reduced. Second, for magnetic shielding structures made of soft magnetic materials, there should be no openings or gaps perpendicular to the direction of the magnetic field lines. If a gap is perpendicular to the magnetic field lines, it will cut the magnetic field lines and increase the magnetic reluctance (i.e., reduce the effectiveness of the magnetic shielding). The permeability μ of the cryogenic Permalloy used in the magnetic shielding of superconducting cavities is closely related to the background magnetic field H. Generally, a background magnetic field of 0–50 mGs (see Fig. 2(b) [FIGURE:2]) is required to maximize the effectiveness of the cryogenic Permalloy magnetic shielding for superconducting cavities. Therefore, creating a weak magnetic field H environment and matching it with the permeability μ to enhance the effectiveness of the magnetic shielding is crucial. In other words, the magnetic shielding around the superconducting cavity alone is not sufficient to effectively shield against all larger background magnetic fields. It is necessary to create an even weaker background magnetic field environment outside the magnetic shielding to provide the prerequisite conditions for achieving high shielding performance.

The factors that affect the background magnetic field around the superconducting cavity magnetic shielding of the module mainly include: (1) The inherent background magnetic field due to the orientation layout of the entire module. The background magnetic field in the east-west direction is significantly smaller than that in the north-south direction. The SHINE cryogenic module is oriented east-west at the ground-level horizontal test station and north-south in the underground tunnel during installation and operation. (2) The effectiveness of the magnetic shielding of the surrounding buildings during module test and operation. The two test stations in Hall 1 of the SHINE ground test station have certain magnetic shielding functions, with an axial background magnetic field in the test space of approximately 150–250 mGs. The two test stations in Hall 2 do not have magnetic shielding functions, with an axial background magnetic field in the test space of approximately 250–350 mGs. The underground north-south tunnel of SHINE is made of reinforced concrete, with an axial background magnetic field of 400–550 mGs at the module installation and operation position. (3) The residual magnetic field of ferromagnetic components, such as stainless steel, within approximately 100 mm around the superconducting cav-

ity, including tuners, couplers, beam pipes, flanges, supports, fastening screws, welded parts, etc. The surface residual magnetic field of these components needs to be strictly controlled before and after installation. According to the SHINE module magnetic field hygiene management regulations, the surface magnetic field of these components should be controlled within 1.0 Gs before installation. If this requirement is not met, demagnetization treatment should be carried out until the requirement is satisfied. The magnetic field of some components increases after installation, especially the surface residual magnetic field of the module' s cryogenic pipeline, which increases significantly after installation and welding. In such cases, online demagnetization is also required to control the magnetic field below the specified value. (4) The level and accuracy of the entire module demagnetization. Although strict magnetic field control was carried out during the installation of the module cryostat and internal components, the module became magnetized to varying degrees during subsequent processes such as installation, integration, debugging, welding, and conditioning. Therefore, it is necessary to perform online in-situ demagnetization of the entire module to reduce the background magnetic field environment of the module cryostat. This paper introduces the experimental situation of online in-situ demagnetization of the entire high-Q module and several engineering modules to create a weak magnetic field H environment.

II. DEMAGNETIZATION EXPERIMENTAL METHOD

The demagnetization of the SHINE cryogenic module essentially involves demagnetizing the vacuum cryostat [14, 15]. Components such as the tuner, coupler, flange, and support pieces around the superconducting cavities inside the module cannot have their residual magnetic fields reduced through whole-module demagnetization. As previously described, these components can only be managed through material selection and individual component demagnetization. Therefore, the demagnetization system and process for the entire module are almost identical to those for the cryostat.

The SHINE module whole machine demagnetization uses the demagnetization system IPS-403E jointly developed with Hunan United Information Security Technology Co., Ltd. The demagnetization system for the whole module consists of two parts: the demagnetization power supply system and the load coil system. The demagnetization power supply system has a total power of about 33 kW, with a demagnetization output current ranging from 6.5 mA to 130 A and a demagnetization frequency of 0.1–1.0 Hz. The switching frequency is switchable between 5 kHz and 10 kHz. It includes an industrial computer, a low-frequency power supply, and a resistor box. The load coil system has a total length of about 1300 m and a total resistance of about 2.0 ohms when connected in series. It uses 12 mm^2 lightweight, high-temperature, and radiation-resistant cables. It includes a 100-turn coil at the module end, 20 groups of coils in the middle (10 turns per group), and output/input leads.

During the SHINE module whole machine demagnetization process, operations such as vacuum pumping, heating, conditioning, and welding, which have varying degrees of impact on demagnetization, need to be avoided. The flowmeter-small range method is used to measure the Q value of individual superconducting cavities or a group of eight superconducting cavities before and after demagnetization, and the results are compared with the vertical test results of the superconducting cavities. The physical appearance of the SHINE cryogenic module to be demagnetized is shown in Fig. 3 [FIGURE:3].

Unlike the demagnetization of cryogenic modules in good insulation from the ground and in isolated conditions, the online in-situ demagnetization of the entire SHINE module in both the horizontal test station and the underground installation and operation states involves connecting numerous signal cables to obtain various data. Additionally, the conductive and magnetic support platform does not employ insulation design measures, resulting in extensive and complex leakage current phenomena at the test station and installation operation sites. This leakage current during the demagnetization process causes unpredictable interference with the online in-situ demagnetization of the entire cryogenic module. Theoretically, disconnecting the leakage current grounding wire before demagnetization could solve the issue of demagnetization interruption or incomplete demagnetization. However, this is not practical in actual operations, as disconnecting the grounding wire would place the module, its associated equipment, and on-site personnel in an unsafe state.

In early 2024, the online in-situ demagnetization of the SHINE high-Q cryogenic module prototype used a non-timed balance mode, which frequently triggered the demagnetization system' s leakage current protection switch, causing unexpected interruptions in the demagnetization process. The non-timed balance mode is not universally applicable for the online in-situ demagnetization of the entire cryogenic module. To address this, subsequent online in-situ demagnetization of the entire SHINE module adopted two demagnetization modes—timed exponential and timed linear—that are less likely to trigger the demagnetization system' s leakage current protection switch. The low-frequency power supply switching frequency was also reduced to minimize interruptions during the online demagnetization process. The current waveforms for the timed exponential and timed linear modes of the SHINE high-Q module demagnetization are shown in Fig. 4

, and the corresponding typical magnetic field waveforms detected by the two fluxgate probes outside the superconducting cavity are shown in Fig. 5 [FIGURE:5]. From the current and magnetic field waveforms, it can be seen that in the timed exponential mode, the current and magnetic field rapidly decay sharply after the initial maximum value, while in the timed linear mode, the current and magnetic field gradually decay according to a linear law after the initial maximum value.

Table 1 shows the demagnetization status of the SHINE high-Q module at different workstations in the installation and test site, including position, current,

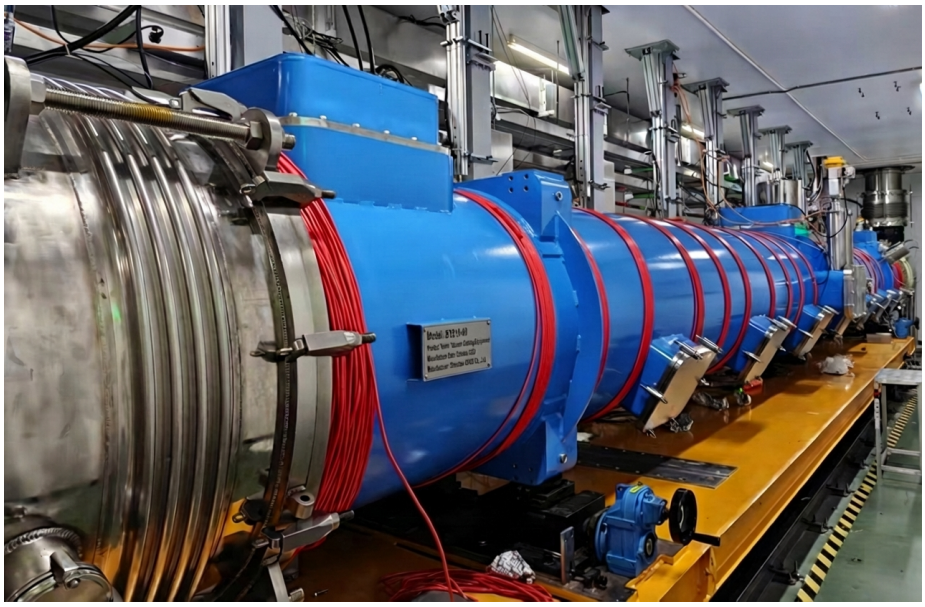

Figure 1: Figure 4

temperature, orientation, etc. To monitor the magnetic field waveform changes and the actual demagnetization results during the online demagnetization process of the SHINE high-Q module, 13 fluxgate probes from Bartington Instruments were strategically placed inside the module [16, 17]. Specifically, CH1, CH12, and CH2 were positioned between the two layers of magnetic shielding outside the titanium jackets of the first, fourth, and fifth cavities, respectively. CH4 was placed horizontally on top of Cell 5 in the first cavity. CH6 and CH7 were positioned at a 45-degree angle on top of Cell 9 and Cell 1 in the fourth cavity, respectively. CH13 and CH14 were placed vertically along the axis at the bottom of Cell 9 and Cell 1 in the fourth cavity, respectively. CH8 and CH9 were positioned at a 45-degree angle on top of Cell 9 and vertically along the axis at the bottom of Cell 9 in the fifth cavity, respectively. CH10 and CH11 were positioned at a 45-degree angle on top of Cell 9 and on top of Cell 1 in the eighth cavity, respectively. CH15 was placed vertically along the axis on top of Cell 9 in the eighth cavity. Notably, to obtain more extreme magnetic field experimental data in this experiment, all ten fluxgate probes inside the cavities, except for CH4, were placed at the two ends of the magnetic shielding cavity where the magnetic field is the strongest. According to the magnetic field simulation results, if the magnetic field at the ends of the magnetic shielding cavity reaches the expected results, the magnetic field in the main area of the magnetic shielding cavity will be even more ideal. This arrangement is shown in Fig. 6

. Similarly, to monitor the magnetic field waveform changes and the actual

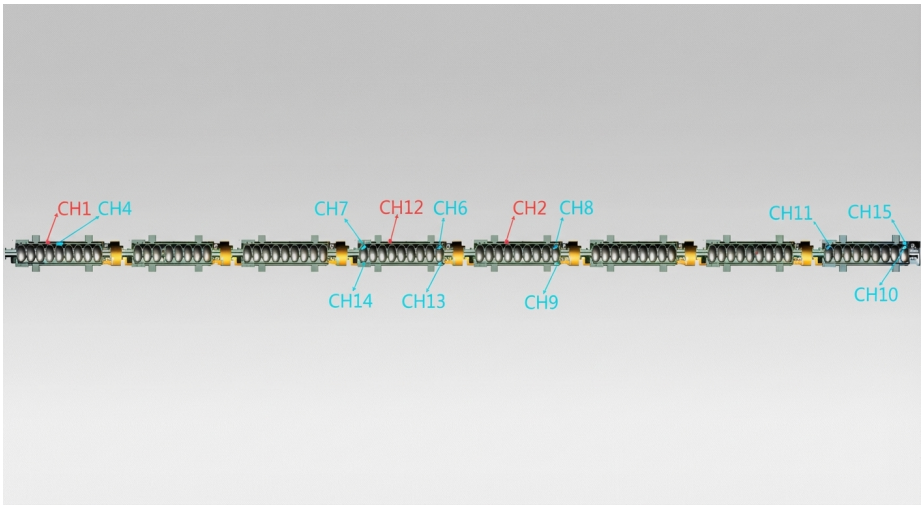

Figure 2: Figure 6

demagnetization results during the online demagnetization process of the engineering module, two fluxgate probes from Bartington Instruments were placed inside the module, between the two layers of magnetic shielding outside the titanium jackets of the first and fifth cavities.

III. DEMAGNETIZATION EXPERIMENTAL RESULTS

3.1 Demagnetization of the High-Q Prototype Module

Fig. 7 [FIGURE:7] illustrates the magnetic field measurements both inside and outside the superconducting cavities before and after the demagnetization of the module. The results show that for the three external fluxgate probes (CH1, CH12, CH2), at the test station in Hall 1, the magnetic fields before demagnetization at 60 A were 0.51 mGs, 2.76 mGs, and 7.59 mGs, respectively. After demagnetization, these values decreased to 0.14 mGs, -0.43 mGs, and -1.09 mGs. When the module was cooled to 2.0 K, the magnetic fields increased slightly but remained lower than before demagnetization. Upon moving the module to the north-south orientation in Hall 1, the magnetic fields for these probes increased significantly, except for CH1, which had faulty data. When the module was relocated to an east-west position away from the test station in Hall 1, the magnetic fields decreased compared to the north-south orientation, but due to environmental magnetic field differences caused by the position change, they increased significantly compared to the demagnetized state. When the module was moved from the ground to the north-south position in the underground tunnel, the magnetic fields for these probes increased significantly again, but

decreased after demagnetization. Finally, when the module was moved from the underground tunnel to the ground in an east-west position, the difference in magnetic fields before and after demagnetization was substantial, with the magnetic fields decreasing dramatically after demagnetization.

For the ten internal fluxgate probes, at the test station in Hall 1, the magnetic fields for CH6, CH7, and CH15 were greater than 5.0 mGs before demagnetization at 60 A. After demagnetization, these values decreased to -1.16 mGs, 0.22 mGs, and 0.14 mGs, respectively, with other probes also showing a decrease in magnetic fields. After cooling to 2 K, the magnetic fields increased slightly overall but remained lower than before demagnetization. When the module was moved to the north-south orientation in Hall 1, the magnetic fields increased significantly for almost all probes. When the module was relocated to an east-west position away from the test station in Hall 1, similar to the external probes, the magnetic fields decreased compared to the north-south orientation, but due to environmental magnetic field differences, they increased significantly compared to the demagnetized state. When the module was moved from the ground to the north-south position in the underground tunnel, the magnetic fields increased significantly for most probes. After demagnetization at 75 A, the magnetic fields decreased, but some probes still had magnetic fields greater than 5.0 mGs. Finally, when the module was moved from the underground tunnel to the ground in an east-west position, the difference in magnetic fields before and after demagnetization was substantial. After demagnetization at 75 A, the magnetic fields inside the module decreased dramatically, with all cavity-internal fluxgate probes showing magnetic fields less than 1.0 mGs. These results demonstrate the effectiveness of the demagnetization process in reducing the magnetic fields both inside and outside the superconducting cavities, achieving the desired weak magnetic field environment for the SHINE high-Q module.

From the results mentioned above, it can be observed that: (1) The demagnetization of the entire module has a significant impact on the magnetic fields both inside and outside the cavity. Essentially, the module should not be moved after demagnetization, as significant changes in the environmental background magnetic field can affect the demagnetization effect. (2) The decrease in temperature after demagnetization causes non-equilibrium thermal currents and other factors, leading to an increase in the magnetic field. (3) The effectiveness of the demagnetization of the entire module is closely related to its orientation. With the same demagnetization current and process parameters, the north-south direction, which has a larger background magnetic field, shows a less effective demagnetization compared to the east-west direction, which has a smaller background magnetic field. (4) The changes in the magnetic fields detected by the fluxgate probes both inside and outside the cavity are generally consistent before and after demagnetization. Since fluxgate probes cannot be placed inside the cavity of the module during operation, placing some fluxgate probes outside the cavity can be used to monitor and trace the changes in the magnetic field inside the cavity before and after demagnetization, providing a reference for operation and maintenance.

Before demagnetization, the average magnetic field values detected by the two fluxgate probes (CH12 and CH2) between the magnetic shielding layers were 5.56 mGs in the east-west direction at the test station in Hall 1, 16.32 mGs in the east-west direction on the ground at Well 2, and 9.42 mGs in the north-south direction at the tunnel entrance of Well 2. The average magnetic field values detected by the ten fluxgate probes (CH4, CH6, etc.) inside the magnetic shielding cavity were 4.03 mGs in the east-west direction at the test station in Hall 1, 4.12 mGs in the east-west direction on the ground at Well 2, and 4.35 mGs in the north-south direction at the tunnel entrance of Well 2. After demagnetization, the average magnetic field values detected by the two fluxgate probes (CH12 and CH2) between the magnetic shielding layers were 0.76 mGs at 60 A demagnetization in the east-west direction at the test station in Hall 1 (1.81 mGs at 2.0 K), 0.94 mGs at 75 A demagnetization in the east-west direction on the ground at Well 2, and 1.90 mGs at 75 A demagnetization in the north-south direction at the tunnel entrance of Well 2. The average magnetic field values detected by the ten fluxgate probes (CH4, CH6, etc.) inside the magnetic shielding cavity were 0.34 mGs at 60 A demagnetization in the east-west direction at the test station in Hall 1 (2.06 mGs at 2.0 K), 0.32 mGs at 75 A demagnetization in the east-west direction on the ground at Well 2, and 1.53 mGs at 75 A demagnetization in the north-south direction at the tunnel entrance of Well 2.

From the data, it can also be seen that the fluxgate probe CH4, located in the main area of the magnetic shielding cavity, had a relatively small magnetic field amplitude throughout the entire process of module movement and before and after demagnetization, with the magnetic field not exceeding 2.0 mGs. The nine fluxgate probes (CH6, etc.) located at the two ends of the magnetic shielding cavity, where the magnetic field is the strongest, had larger changes in magnetic field amplitude throughout the entire process of module movement and before and after demagnetization, with some positions having magnetic fields close to or exceeding 5.0 mGs. After the first demagnetization of the SHINE high-Q module, the magnetic field was less than 1.0 mGs overall, which is better than the demagnetization results of similar modules in the United States LCLS-II, where the magnetic field after demagnetization in the east-west direction was less than 2.3 mGs [18].

Fig. 8 [FIGURE:8] shows the Q test results of the SHINE high-Q module before and after online demagnetization. The observations are as follows: (1) For the entire module, the Q values of CAV1, CAV6, and CAV7 were 2.70×10^{1}, 2.50×10^{1}, and 2.93×10^{1}, respectively, before demagnetization. After demagnetization, these values increased significantly to 3.27×10^{1}, 3.28×10^{1}, and 3.09×10^{1}, respectively. When demagnetization was interrupted in the non-timed balance mode (equivalent to the module being magnetized), the Q values of these three superconducting cavities dropped dramatically to 2.14×10^{1}, 1.11×10^{1}, and 0.76×10^{1}, respectively. This indicates that the magnetic field inside the magnetic shielding structure of the superconducting cavities has a significant impact on Q. (2) Other cavities, such as CAV5 and CAV8, also saw substan-

tial improvements in Q after demagnetization. The Q values of CAV2, CAV3, and CAV4 reached the design target of 2.7×10^{1} after demagnetization, with CAV2 achieving a Q of 5.36×10^{1}. This improvement may be due to a more noticeable reduction in the magnetic field within the cavity, as well as the inherent performance of the cavity itself. (3) For the overall Q measurement (eight cavities, 134.5 MV), the Q values before and after demagnetization were 2.58×10^{1} and 3.32×10^{1}, respectively. The post-demagnetization value met the key acceptance criteria for Q of the entire module. These results demonstrate the significant impact of demagnetization on improving the Q of the superconducting cavities in the SHINE high-Q module, highlighting the importance of effective magnetic field control for achieving optimal performance.

3.2 Demagnetization of High-Q Application Modules

Table 2 shows the changes in the average absolute magnetic field values detected by the two fluxgate probes between the magnetic shielding layers before and after demagnetization, as well as the test results for the key indicator Q for subsequent similar application modules. For 12 eight-cavity 1.3 GHz modules, the magnetic field between the magnetic shielding layers significantly decreased to 0.20–0.50 mGs after demagnetization, indicating that the magnetic field in the main area of the superconducting cavities would be even smaller. Except for CM02, the key indicator Q for all modules generally met the design specifications. The failure of CM02 to meet the expected results may be closely related to the relatively low demagnetization current, the inherent performance of the superconducting cavities, and quenching during the test process.

Among the 12 standard 1.3 GHz engineering modules that underwent demagnetization, CM01, CM02, CM03, CM04, CM05, CM06, CM07, and CM08 used the timed exponential mode for demagnetization, with the magnetic field between the magnetic shielding layers controlled at 0.20–0.50 mGs after demagnetization. CM09, CM10, CM11, and CM12 used the timed linear mode for demagnetization, with the magnetic field between the magnetic shielding layers controlled below 0.20 mGs, slightly better than the timed exponential mode.

For module CM01, the Q changes before and after demagnetization were tested for each superconducting cavity, as shown in Fig. 9 [FIGURE:9]. It can be observed that the Q of almost all superconducting cavities increased to varying degrees after demagnetization. During the Q test process after demagnetization, quenching of the superconducting cavities had a significant impact on the results. Generally, compared to vertical test, the Q values of superconducting cavities without quenching were higher. Among them, the Q values of CM01 and CM08 were much higher than those obtained from vertical test. Except for CM05, the ratio of horizontal test to vertical test Q values for other superconducting cavities exceeded 90%. In contrast, CM02, CM07, and CM09 experienced quenching to varying degrees during the Q test process after demagnetization, resulting in much lower Q values for these modules.

According to Fig. 1, the magnetic field in the main area of the superconducting cavities after demagnetization of modules CM01-CM12 is expected to be controlled at the 0.50 mGs level. Theoretically, the Q of all superconducting cavities should approach 4.0×10^{1}. However, in practice, only the Q values of CM01, CM06, and CM08 are close to 4.0×10^{1}. This indicates that other factors, such as quenching during test and the inherent performance of the cavities, may also have a significant impact on the Q of the superconducting cavities.

Module CM10 attempted an online demagnetization method under a low-temperature operating environment at 41 K. As shown in Fig. 10

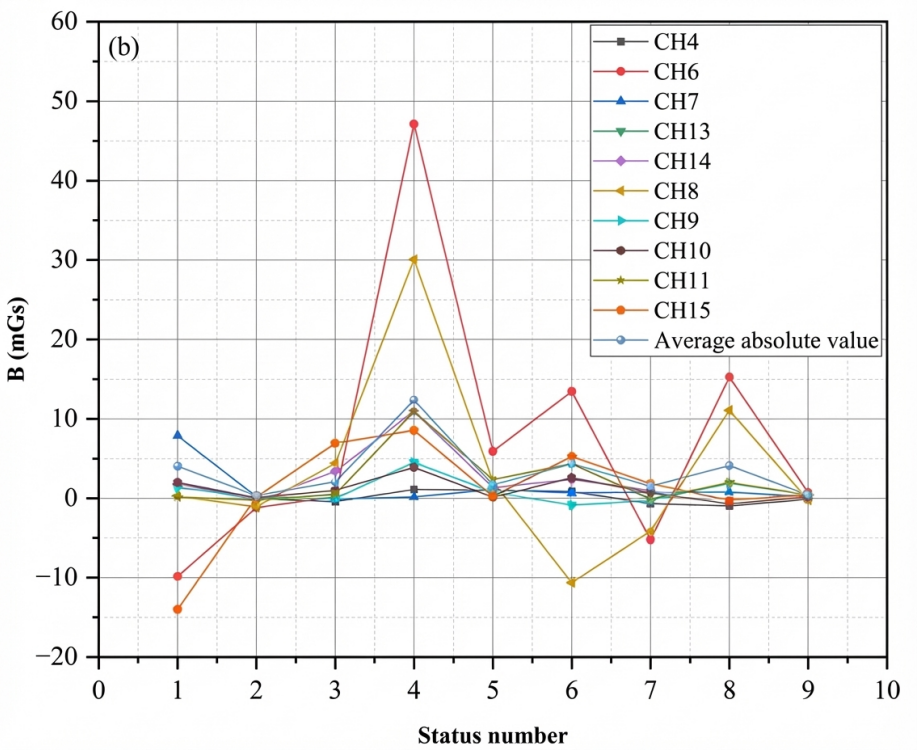

Figure 3: Figure 10

, there is a significant difference in the Q of the entire module before and after demagnetization, with values of 2.41×10^{1} at 112 MV before demagnetization and 3.37×10^{1} at 112 MV after demagnetization. The overall results obtained from low-temperature demagnetization are consistent with those from room-temperature demagnetization. However, microthermal currents inside the superconducting cavities during low-temperature demagnetization have an adverse effect on the Q results, although the magnitude of this effect should be relatively small. After online demagnetization, the Q test of module CM10 did not experience quenching in the superconducting cavities. The ratio of the Q

value obtained from the horizontal test to that from the vertical test was 84%, which is lower than the expected 90%. Whether this discrepancy is related to the presence of thermal currents during low-temperature demagnetization remains to be determined. Further experience data needs to be accumulated and analyzed to provide a more comprehensive understanding.

IV. DISCUSSION AND CONCLUSIONS

This paper presents the results of online in-situ demagnetization of the SHINE high-Q module prototype and demonstrates that the background magnetic field and demagnetization current of the entire module have a significant impact on the demagnetization outcome. After online demagnetization, the magnetic field B inside the superconducting cavities can be controlled at the 0.20–0.50 mGs level, with Q values reaching 2.7×10^{1} to 5.3×10^{1}. These results meet the key performance requirements of the SHINE module and are superior to similar online demagnetization outcomes from international counterparts. The Q values of different superconducting cavities after demagnetization show significant variation, which may be related not only to the magnetic field but also to the performance of the cavities themselves and the occurrence of quenching during testing. The magnetic field changes detected by the fluxgate probes outside and inside the cavities are almost consistent before and after demagnetization. Therefore, fluxgate probes can be placed outside the cavities during module installation and operation to monitor the demagnetization process.

To reduce the workload and improve the results of demagnetization, the background magnetic field should remain stable after online in-situ demagnetization of the entire module. When demagnetizing in the north-south direction, a higher demagnetization current is required to achieve the same effect as in the east-west direction, indicating that demagnetization in the north-south direction is more challenging. After demagnetization, operations that may affect the demagnetization outcome, such as transportation, welding, conditioning, and vibration, should generally be avoided. Essentially, these operations can lead to re-magnetization of the module.

Worth exploring and researching is the underlying mechanism of the occasional interruption phenomenon in the non-timed balance mode of online demagnetization for the entire module, while also paying attention to whether the timed exponential and timed linear modes do not experience demagnetization interruptions under more complex leakage magnetic conditions. Compared to the timed exponential mode, the timed linear mode has a longer demagnetization time at higher currents, allowing the stubborn high Hc magnetic domains in the module cryostat material to be more thoroughly randomized. Theoretically, this results in a more complete demagnetization, which has been preliminarily verified in the demagnetization results of modules CM09, CM10, CM11, and CM12. Further accumulation and analysis of demagnetization data from appli-

cation modules are needed to understand the differences between the two timed modes.

The demagnetization results of the entire module are closely related to the background magnetic field of the test station or operational state. Except for CM10, the demagnetization of high-Q modules and 12 application modules has been carried out at two positions in Hall 1 with a smaller background magnetic field and relatively simpler leakage current. In positions with a larger background magnetic field and more complex leakage current in Hall 2, and in the underground tunnel with an even larger background magnetic field in the north-south direction, the demagnetization results of the entire module may vary to some extent. The corresponding demagnetization process parameters may need to be optimized to achieve better results.

Before demagnetization, the magnetic field in the main area inside the superconducting cavities of the SHINE module generally meets the requirement of being less than 3.0 mGs. However, based on the actual Q test results, controlling the magnetic field inside the superconducting cavities at 3.0 mGs may not be sufficient. The magnetic field inside the superconducting cavities after demagnetization of the entire module needs to be controlled below 1.0 mGs or even 0.50 mGs to achieve better Q performance. Based on the low-temperature demagnetization results of CM10, there is little difference between low-temperature and room-temperature demagnetization, but neither has achieved better results. Further accumulation of low-temperature demagnetization data and analysis are needed.

REFERENCES

[1] Hard X-ray Free Electron Laser Facility. Project profile, http://shine.shanghaitech.edu.cn/; 2025 [accessed 18 January 2025]

[2] Shanghai Large Advanced Cluster. Light Cluster Source project, http://www.sari.cas.cn/lari/jqxm/lariyxsxzu/; 2025 [accessed 14 April 2025]

[3] Z. Qi, N.S. Huang, H.X. Deng, et al. Research on the performance parameters and stability of the Shanghai hard X-ray free-electron laser facility. Acta Optica Sinica 42(11): 1-8 (2022). https://doi.org/10.3788/AOS202242.1134016

[4] A. Grassellino, A. Romanenko, D. Sergatskov, et al. Nitrogen and argon doping of niobium for superconducting radio frequency cavities: a pathway to highly efficient accelerating structures. Supercond. Sci. Technol. 26, 102001 (2013).

[5] D.A. Gonnella, The fundamental science of nitrogen-doping of niobium superconducting cavities. (Cornell University; 2016)

[6] G Wu. Overview on magnetic field management and shielding in high Q modules. In Proc. 17th Int. Conf. on RF Superconductivity (SRF' 15) 2015 Sep.

[7] A. Romanenko and A. Crawford, Magnetic Shielding: Requirements and Possible Solutions, LCLSII Engineering Note, LCLSII-4.5-EN-0222.

[8] P. Hasan, K. Jens, H. Tom, RF Superconductivity for Accelerators. (New York: Cornell University Ithaca, 1998), pp. 6-7.

[9] H.M. Wen, L.G. Yan, L.Z. Lin. Status of superconductivity in large-scale particle accelerators. Cryo. Supercond. 1: 46-49 (2005). https://doi.org/10.16711/j.1001-7100.2005.01.011

[10] J. Theilacker. 1.3 GHz superconducting RF cryomodules. Functional Requirements Specification Document, LCLSII-4.5-FR-0053.

[11] T. Peterson, "1.3 GHz Cryomodule Technical Description," Engineering Specification Document, LCLS-II-4.5-ES-

[12] S.K. Chandrasekaran, K. Saito, S. Shanab, et al. Magnetic shield material characterization for the facility for rare isotope beams'cryomodules. IEEE Trans. Appl. Supercond. 25(3): 1-5 (2014). https://doi.org/10.1109/TASC.2014.2375192

[13] F.Y. Sun, Dissertation, (Integrated Circuit Engineering, Xi' an University of Technology, 2018).

[14] A.C. Crawford, A study of magnetic shielding performance of a fermilab international linear collider superconducting rf cavity cryomodule (2014). arxiv:1409.0828.

[15] M. Masuzawa, N. Ohuchi, A. Terashima, et al. Study of magnetic shield for the STF cryomodules. IEEE Trans. Appl. Supercond. 18(2): 1423-1426 (2008). https://doi.org/10.1109/TASC.2008.921943

[16] S.K. Chandrasekaran, C. Ginsburg. LCLS-II CM Ambient Field Management. TTC meeting, Saclay, France, July 2016.

[17] S.K. Chandrasekaran. Demagnetization of a Fully Assembled LCLS-II Cryomodule (to be published).

[18] S.K. Chandrasekaran, A. C. Crawford. Demagnetization of a Complete Superconducting Radiofrequency Cryomodule: Theory and Practice. IEEE Trans. Appl. Supercond. 27(1): 1-6 (2017). https://doi.org/10.1109/TASC.2016.2635803

Table 1 . Demagnetization status of the entire high-Q module of SHINE.

Module position	Demagnetization current	Measure status
Hall 1 test station	60 A	293K before demagnetization

Module position	Demagnetization current	Measure status
Hall 1 test station	60 A	293K after demagnetization
Hall 1 test station	60 A	2K after demagnetization
Hall 1 north-south direction	75 A	293K after demagnetization
Hall 1 east-west direction	75 A	293K after demagnetization
Well 2 underground north-south demagnetization	75 A	293K before demagnetization
Well 2 underground north-south demagnetization	75 A	293K after demagnetization
Well 2 ground north-south direction	75 A	293K before demagnetization
Well 2 ground north-south direction	75 A	293K after demagnetization

Table 2 . Q Test Results After Demagnetization of SHINE Application Modules.

Module number	Position	Demagnetization mode/current	Magnetic field before/after demagnetization	H/V Q	Whether quenching
CM01	Hall 1	Timed exponential mode/75 A	2.00 mGs/0.20 mGs	3.51 × 10^1 @133 MV	120%
CM02	Hall 1	Timed exponential mode/60 A	1.00 mGs/0.30 mGs	2.63 × 10^1 @166 MV	86%
CM03	Hall 1	Timed exponential mode/75 A	1.77 mGs/0.50 mGs	3.87 × 10^1 @166 MV	98%
CM04	Hall 1	Timed exponential mode/75 A	0.80 mGs/0.40 mGs	3.14 × 10^1 @166 MV	91%

Module number	Position	Demagnetization mode/current	Magnetic field before/after demagnetization	H/V Q	Whether quench-ing
CM05	Hall 1	Timed exponential mode/75 A	2.00 mGs/0.25 mGs	3.13 × 10^1 @166 MV	82%
CM06	Hall 1	Timed exponential mode/75 A	1.40 mGs/0.30 mGs	4.05 × 10^1 @166 MV	99%
CM07	Hall 1	Timed exponential mode/75 A	2.40 mGs/0.20 mGs	2.87 × 10^1 @166 MV	68%
CM08	Hall 1	Timed exponential mode/75 A	0.35 mGs/0.29 mGs	4.21 × 10^1 @166 MV	108%
CM09	Hall 2	Timed linear mode/75 A	0.34 mGs/0.18 mGs	3.14 × 10^1 @165 MV	78%
CM10	Hall 1	Timed linear mode/75 A	1.40 mGs/0.19 mGs	3.37 × 10^1 @112 MV	84%
CM11	Hall 1	Timed linear mode/75 A	0.35 mGs/0.15 mGs	3.07 × 10^1 @166 MV	78%
CM12	Hall 1	Timed linear mode/75 A	0.25 mGs/0.16 mGs	3.41 × 10^1 @163 MV	81%

The authors would like to express their gratitude to the SHINE module development team for their support in experimental test.

† Corresponding author, heyz@sari.ac.cn